Obrabotka metallov (tekhnologiya, oborudovanie, instrumenty) = Metal Working and Material Science. 2023 vol. 25 no. 1 pp. 57–70
ISSN: 1994-6309 (print) / 2541-819X (online)
DOI: 10.17212/1994-6309-2023-25.1-57-70

NSTU NETI

Obrabotka metallov -
Metal Working and Material Science

Journal homepage: http://journals.nstu.ru/obrabotka_metallov

Simulation of the relationship between input factors and output indicators of the internal grinding process, considering the mutual vibrations of the tool and the workpiece

Sergey Bratan [a, *], *Anastasia Chasovitina* [b]

Sevastopol State University, 33 Universitetskaya str., Sevastopol, 299053, Russian Federation

[a] https://orcid.org/0000-0002-9033-1174, serg.bratan@gmail.com, [b] https://orcid.org/0000-0001-6800-9392, nastya.chasovitina@mail.ru

ARTICLE INFO

Article history:
Received: 23 December 2022
Revised: 14 January 2023
Accepted: 25 January 2023
Available online: 15 March 2023

Keywords:
Grinding of titanium
Vibrations
Mutual vibrations
Pinholes
Processing modes
Balance of movements in the technological system

Acknowledgements
Research were conducted at core facility "Structure, mechanical and physical properties of materials".

ABSTRACT

Introduction. In real production conditions, the technological modes recommended in the scientific literature do not reflect the declared qualities, due to the fact that it does not take into account many factors inherent in the process of finishing grinding, for example, its stochastic nature, changes in its dynamic properties, an increase in mutual vibrations of the tool and the workpiece that appear due to changes in the state of the technological system, for example, an increase in vibrations machine tool due to uneven tool wear, etc. All previously developed models have a limited scope of application, it does not take into account the fact that the appearance of vibrations leads to fluctuations in the depth of grinding, with accidental contact of grains with the material being processed, where one group of grains cuts off the material, the other gets into the trace of scratches left by previous grains, etc. This leads to changes in the values of material removal, surface roughness and other parameters of the technological system, which directly affects the accuracy of processing and the quality of the machined surfaces. **The purpose of the work** is to develop mathematical models that establish the relationship between the processing modes and the current parameters of the contact zone during the fine grinding of pinholes, taking into account the mutual vibrations of the tool and the workpiece. **The research methods** are mathematical simulation using the basic provisions of the theory of abrasive-diamond processing. **Results and discussion.** The interrelations between the cutting modes and the current input parameters of the contact zone when grinding pinholes are established, taking into account the mutual vibrations of the tool and the workpiece, which make it possible to determine the parameters of the system at the output to avoid cost losses, including reducing the number of defective products and time costs. Non-stationary mathematical dependences are constructed that allow determining the cutting modes during the implementation of the grinding cycle, taking into account the magnitude of relative vibrations and the initial phase. It is established that instead of a steady process, harmonic oscillations are observed caused by deviations in the shape of the circle, the intensity of tool wear and other factors, all of the above has a significant impact on the quality of the machined surface. The obtained models are universal for various characteristics of the tool, however, for a more adequate description of the process, mathematical dependencies are needed that take into account the wear of the tool on various binders, which is the task of further research.

For citation: Bratan S.M., Chasovitina A.S. Simulation of the relationship between input factors and output indicators of the internal grinding process, considering the mutual vibrations of the tool and the workpiece. *Obrabotka metallov (tekhnologiya, oborudovanie, instrumenty) = Metal Working and Material Science*, 2023, vol. 25, no. 1, pp. 57–70. DOI: 10.17212/1994-6309-2023-25.1-57-70. (In Russian).

Introduction

To date, the machine-building industry implements many methods of processing materials with high accuracy, including ultrasonic and laser processing, high-speed milling processes, as well as abrasive-diamond processing operations, and specifically the internal grinding process. The grinding process has become widespread due to high efficiency, low costs, along with its accuracy and the quality of the processed surface layer [1–7].

*** Corresponding author**
Bratan Sergey M., D. Sc. (Engineering), Professor
Sevastopol State University
33 Universitetskaya str,
299053, Sevastopol, Russian Federation
Tel.: +7 (978)7155019, **e-mail:** serg.bratan@gmail.com

Despite the wide variety of models describing the processes of abrasive diamond processing, there are practically no scientifically-based recommendations in the modern literature that make it possible to guarantee the receipt of the specified product quality parameters in non-stationary conditions of the technological process [8–12]. Therefore, a comprehensive study of the regularities of the surface geometry generation processes, the development of mathematical models will ensure the creation of highly efficient technological processes and optimal designs of abrasive tools on this basis.

The analysis of works in the field of grinding theory allows concluding that all existing models of abrasive-diamond machining processes can be divided into two classes. The first class (*pulse models*) includes mathematical dependencies that simulate the impact of single abrasive grains on the workpiece. The processed surface is formed as a set of grain traces, which in a section perpendicular to the direction of the cutting speed are identical to the profile of the radius of the vertex of the abrasive grain, for example, mathematical models, developed by *I.M. Brozgol*, *D.V. Korolev*, *E.N. Maslov*, *Yu.K. Novoselov*, *V.A. Nosenko* and others [13–17].

The second class (*geometric models*) includes mathematical dependencies that simulate the effect on the workpiece by a set of elementary cutting profiles. On this basis, work has been carried out on the mechanisms of surface roughness formation, for example, mathematical models developed by *Yu.R. Witenberg*, *Yu.V. Linnik*, *S.A. Popov*, *V.A. Shchegolev*, *A.P. Husu* and other scientists [18–23].

In real production conditions, the technological modes, recommended in the above-reviewed works, and reference literature do not reflect the declared qualities, due to the fact that it does not take into account many factors inherent in the process of finishing grinding, for example, its stochastic nature, changes in its dynamic properties, an increase in mutual vibrations of the tool and the workpiece, which appear due to changes in the state of the technological system, for example, an increase in machine vibrations due to uneven tool wear, etc. All previously developed models have a limited scope of application, it does not take into account the fact that the appearance of vibrations leads to fluctuations in the depth of grinding, with accidental grains contact with the material being processed, where one group of grains cuts off the material, the other falls into the trace of scratches left by previous grains, etc. This leads to changes in the values of material removal, surface roughness and other parameters of the technological system, which directly affects the accuracy of processing and the quality of the processed surfaces. To compensate for calculation errors in real production conditions, various technological approaches are used, for example, tools with soft binders are used, feed rates are reduced and other methods are used, which reduce the efficiency of the operation and increases the cost of manufactured products.

Advanced approach to problem is to continue research of grinding operations, (in particular internal), in the course of which it is necessary to identify and describe the relationship between input factors and output indicators of the process.

Based on the established relationships, it is necessary to build mathematical models that adequately simulate the grinding process, taking into account the mutual vibrations of the tool and the workpiece.

To date, one of the most time-consuming technological processes is the grinding operation. The amount of products where internal grinding was used as a finishing machining is not inferior to the amount of products, processed by the external method. However, internal grinding is more difficult due to the heavy flow of the machining process and the lower rigidity of the cutting tools.

In connection with the above, the purpose of this paper is to develop mathematical models that establish the relationship between the working modes and the current parameters of the contact zone during fine grinding of precise holes, taking into account the mutual vibrations of the tool and the workpiece.

Research methodology

The scheme of the finishing process of the hole (internal grinding) is shown in Fig.

After inserting a workpiece into a chuck, the tool and the workpiece are set to rotate at a circumferential speed V_u and V_k accordingly. When moving the grinding head in the direction of radial feed S_y, the difference between the radius vectors of the workpiece and the tool becomes less than the center distance A_i, and an area of interpenetration of the tool into the workpiece material – *the contact zone* – is formed [24].

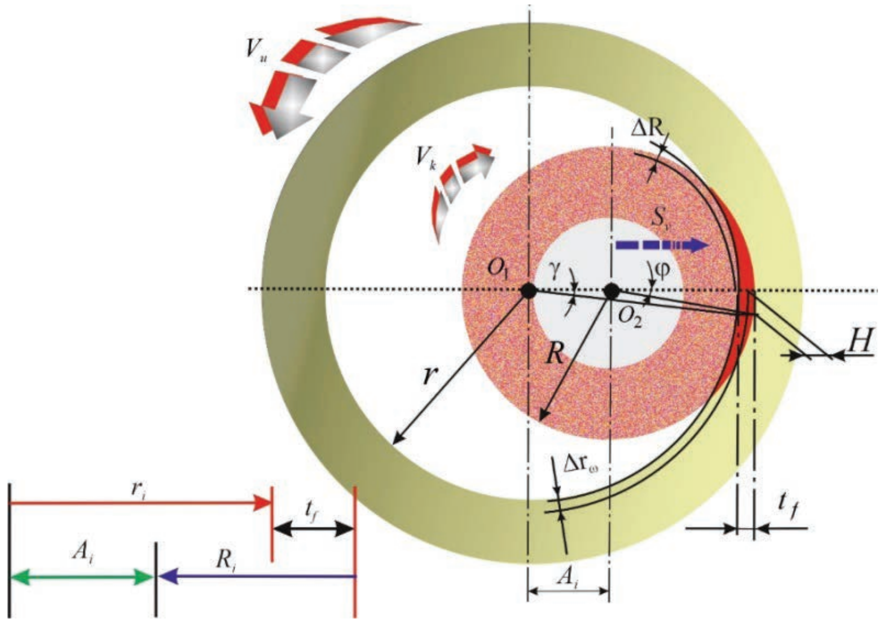

Internal grinding process scheme

In accordance with the dimensional scheme of the internal grinding process, shown in Fig., the displacement balance equation takes the form:

$$\Delta A_i = S_{yi} + N = \Delta t_{fi} - \Delta R_i + \Delta r_{\omega i-1} + \Delta A_{yi}\,, \tag{1}$$

where ΔA_i – current changes in the value of the center-to-center distance, due to the radial feed of the grinding head, m; S_{yi} – radial tool feed, m; N – preload, m; Δt_{fi} – changing the actual cutting depth, m; ΔR_i – current tool wear, m; $\Delta r_{\omega i-1}$ – the amount of material removed before the current revolution, m; ΔA_{yi} – current change in elastic deformations.

During internal grinding, an uneven removal of the allowance is observed, a waviness is formed on the surface of the workpiece [25, 26]. Based on this, it can be assumed that not only the removal of the allowance will change according to the harmonic law, but also other parameters included in the balance equation of displacements.

For a visual demonstration of this phenomenon, the processing cycle by solving the displacement balance equation will be calculated [27, 28]. **Initial data:** the material of the workpiece is titanium alloy *VT3*, d = 150 mm, grinding head *AW 60×25×13 63C F90 M 7 B A 35 m/s* , circumferential speed of the wheel V_k = 35m/s, workpiece speed V_u = 0.25 m/s, radial feed S_{ui} = 0.005 mm/r, number of grains per unit area n_g = 15.86·106 pcs/m^2, corner radius the grain vertex $\rho_g = 7.31\cdot10^{-6}$ m).

Results and its discussion

When calculating the parameters of the penetration stage, the values of the transverse feed $S_{y1} = 5\cdot10^{-6}$ m and preload $N = 10\times10^{-6}$ m are preset, according to the values, given in the reference literature [16].

Let's perform the calculation of the first revolution:

1) Find the sum of the parameters of preload and cross feed:

$$\Delta A_1 = S_{y1} + N = 5\cdot10^{-6} + 10\cdot10^{-6} = 15\cdot10^{-6}, \text{ m}$$

2) Determine the increment of elastic deformations in accordance with the equation:

$$\Delta A_{yi} = \omega_{TS}\cdot\Delta P_y\,, \tag{2}$$

where ω_{TS} is a system compliance; $\omega_{TS} = 30\cdot10^{-9}$ m·N; ΔP_y is increment of the normal component of the cutting force; $\Delta P_y \geq 0$.

Let's assume that there is no increment of the normal component of the cutting force at the first revolution $\Delta P_y = 0$, therefore, after substituting the parameter values into the formula, we get:

$$\Delta A_{y1} = 0 \text{ , m}$$

3) Calculate the depth of micro-cutting.

On the previous revolution, there is no radial removal of the material $\Delta r_0 = 0$.

Given the assumption that the wear of the grinding wheel on the first revolution is equal to zero, $\Delta R_1 = 0$, then the equation (1) is defined as:

$$\Delta A_1 = \Delta t_{f1} = 15\cdot10^{-6} \text{ , m}$$

From here, the value of the depth of micro-cutting is calculated:

$$t_{f1} = S_{y1} + \Delta t_{f1} = 0 + 15\cdot10^{-6} = 15\cdot10^{-6} \text{ , m}$$

4) At the current revolution, the value of the radial removal of the material can be determined by the equation:

$$\Delta r_{\omega i} = \frac{t_{fi}^{2}}{\frac{7\pi}{15}t_{fi} + \frac{13\pi}{3}\frac{V_u}{K_c(V_k + V_u)n_g\sqrt{D_e\rho_g}} + |\Psi|^{0,4}}, \tag{3}$$

where K_c – chip formation coefficient, $K_c = 0.85$; V_u – the speed of rotation of the workpiece, m/s; V_k – the speed of rotation of the wheel, m/s; n_g – number of grains per unit area, pcs/m^2; ρ_g – corner radius the grain vertex, m; D_e – equivalent diameter, m.

The equivalent diameter is calculated by the equation:

$$D_e = \frac{D\cdot d}{D - d}, \tag{4}$$

where D – diameter of the grinding wheel, m; d – the diameter of the workpiece, m.

After substituting the data into equation (4), we get:

$$D_e = \frac{150\cdot60}{150 - 60} = 0.1 \text{ , m.}$$

The value of the variable Ψ it will be calculated depending on the initial phase of the deviations.

For $\psi_y = 0\times(2\pi)$ and $\psi_y = \pi$:

$$\Psi = \frac{15}{16}A_\omega{}^2\sqrt{t_f} + \frac{15A_\omega{}^2V_u\sin2\gamma}{32\omega D_e{}^{0,5}} + \frac{15A_\omega V_u{}^3\sin\gamma}{2D_e{}^{1,5}\omega^3} + \frac{15A_\omega V_u{}^2\sqrt{t_f}\left(2\sin\left(\frac{\gamma}{2}\right)^2 - 1\right)}{2D_e\omega^2}$$

or

$$\Psi = \frac{15}{16}A_\omega{}^2\sqrt{t_f} + \frac{15A_\omega^2V_u\sin2\gamma}{32\omega D_e{}^{0,5}} + \frac{15A_\omega V_u{}^3\sin\gamma}{2D_e{}^{1,5}\omega^3} + \frac{15A_\omega V_u{}^2\sqrt{t_f}\sqrt{1-\sin^2(\gamma)}}{2D_e\omega^2},$$

If $\psi_y = \pi/2$ and $\psi_y = 3\pi/2$:

$$\Psi = \frac{15}{16}A_\omega^2\sqrt{t_f} - \frac{15A_\omega^2V_u\sin2\gamma}{32\omega D_e{}^{0,5}},$$

where A_ω – amplitude, μm; ω – cyclic frequency, rad/s; ψ_y – the initial phase of vibrations; variable $\gamma = \dfrac{\omega \cdot (t_f - y)^{0,5} \cdot D_e^{0,5}}{V_u}$, where y – the level in question.

At the initial phase of relative fluctuations $\psi_y = 0\times(2\pi)$ and amplitude $A_\omega = 0.2\times t_{fi}$, $\omega = 628$ rad/s material removal at the current speed, taking into account vibrations:

$$\Delta r_{\omega 1} = \frac{(15 \cdot 10^{-6})^2}{\dfrac{7\pi}{15} 15 \cdot 10^{-6} + \dfrac{13\pi}{3} \dfrac{0,25}{0.85(35 + 0.25)15.866 \cdot 10^6 \sqrt{0.1 \cdot 7.31 \cdot 10^{-6}}} + \left|0.17 \cdot 10^{-12}\right|^{0,4}} = 5.89 \cdot 10^{-6}\text{, m}$$

5) Calculate the thickness of the surface layer, in which the roughness is located, according to:

$$H_i = t_{fi} - \Delta r_{\omega i}, \tag{5}$$

When substituting parameter values into equation (5), we get:

$$H_i = t_{fi} - \Delta r_{\omega i} = 15 \cdot 10^{-6} - 5.89 \cdot 10^{-6} = 9.11 \cdot 10^{-6}\text{, m.}$$

6) Calculate the cutting force as follows:

$$P_{yi} = 3\sqrt{2} L_k n_g \sqrt{\rho_g h_{g\max} H_i D_e} \left(0.055 H_i \frac{\sin\beta}{\sin\beta_1} + 0.061\sqrt{\rho_g h_{g\max}}\right)\tau_s, \tag{6}$$

where L_k – grinding wheel height, m; $h_{g\max}$ – grain wear, $h_{g\max} = 10\cdot 10^{-6}$ m; β and β_1 – cutting angles of abrasive material, β = 22° and β_1 = 34°; τ_s – shear stress, N/m^2.

The shear stress is defined as:

$$\tau_s = \frac{\sigma}{1,5}, \tag{7}$$

where σ – ultimate strength of the material, $\sigma = 2\cdot 10^9$ N/m^2,

$$\tau_s = \frac{2 \cdot 10^9}{1.5} = 13.33 \cdot 10^8\text{, N/m}^2$$

By substituting the data into equation (6), the cutting force is determined as:

$$P_{y1} = 3\sqrt{2} \cdot 25 \cdot 10^{-3} \cdot 15.866 \cdot 10^6 \sqrt{7.31 \cdot 10^{-6} \cdot 10 \cdot 10^{-6} \cdot 9.11 \cdot 10^{-6} \cdot 0.1} \times$$

$$\times \left(0.055 \cdot 9.11 \cdot 10^{-6} \cdot \frac{0.3746}{0.5591} + 0.061\sqrt{7.31 \cdot 10^{-6} \cdot 10 \cdot 10^{-6}}\right) \cdot 13.33 \cdot 10^8 = 2.899\text{, N.}$$

7) Clarify previously obtained calculated values Δt_{f1}, Δr_1, P_{y1}.

The value of the increment of elastic deformations is determined as:

$$\Delta A_{y1} = \omega_{TS} \cdot \Delta P_y = \omega_{TS} \cdot (P_{y1} - P_{y0}) = 30 \cdot 10^{-9} \cdot (2.899 - 0) = 8.698 \cdot 10^{-8}\text{, m.}$$

The micro-cutting depth' increment and the micro-cutting depth values are calculated, respectively as follows:

$$\Delta t_{f1} = \Delta A_1 - \Delta A_{y1} = 15 \cdot 10^{-6} - 8.698 \cdot 10^{-8} = 14.91 \cdot 10^{-6}\text{, m,}$$

$$t_{f1} = t_{f0} + \Delta t_{f1} = 0 + 14.91 \cdot 10^{-6} = 14.91 \cdot 10^{-6}\text{, m.}$$

The amount of material removal will be:

$$\Delta r_{\omega 1} = \frac{(14.91 \cdot 10^{-6})^2}{\frac{7\pi}{15} 14.91 \cdot 10^{-6} + \frac{13\pi}{3} \frac{0.25}{0.85 \cdot (35 + 0.25) \cdot 15.866 \cdot 10^6 \sqrt{0.1 \cdot 7.31 \cdot 10^{-6}}} + \left|0.17 \cdot 10^{-12}\right|^{0,4}} = 5.844 \cdot 10^{-6}\text{, m}$$

The thickness of the layer in which the roughness is distributed:

$$H_1 = t_{f1} - \Delta r_{\omega 1} = 14.91 \cdot 10^{-6} - 5.844 \cdot 10^{-6} = 9.069 \cdot 10^{-6}\text{, m}$$

The cutting load:

$$P_{y1} = 3\sqrt{2} \cdot 25 \cdot 10^{-3} \cdot 15.866 \cdot 10^6 \sqrt{7.31 \cdot 10^{-6} \cdot 10 \cdot 10^{-6} \cdot 9.069 \cdot 10^{-6} \cdot 0.1} \times$$

$$\times \left(0.055 \cdot 9.069 \cdot 10^{-6} \frac{0.3746}{0.5591} + 0.061\sqrt{7.31 \cdot 10^{-6} \cdot 10 \cdot 10^{-6}}\right) 13.33 \cdot 10^8 = 2.884\text{ , N.}$$

8) The distance from the deepest valley to the midline of the profile is calculated according to:

$$W_{mi} = \frac{t_{fi} - \Delta r_{\omega i}}{2}. \tag{8}$$

Insert numeric values into the equation (8):

$$W_{m1} = \frac{14.91 \cdot 10^{-6} - 5.844 \cdot 10^{-6}}{2} = 4.535 \cdot 10^{-6}\text{, m}$$

One of the final stages of calculating the parameters of the revolution under consideration is the comparison of the value W_{m1} with the amount of $\Delta r_{\omega 1}$,

$$W_{m1} \le \Delta r_{\omega 1}$$

$$4.535 \times 10^{-6} \le 5.844 \cdot 10^{-6}.$$

Due to the fact that the value of $\Delta r_{\omega 1}$ exceeds the value of W_{m1}, then the value of the arithmetic mean length of the profile R_a is determined as:

$$R_a = \frac{0.25 V_u^{0.4} t_{f1}^{0.6}}{K_c (V_u + V_k)^{0.4} n_g^{0.4} D_e^{0.2} \rho_g^{0.2}} =$$

$$= \frac{0.25 \cdot 0.25^{0,4} (14.91 \cdot 10^{-6})^{0.6}}{0.85^{0.4} (0.25 + 35)^{0.4} (15.866 \cdot 10^6) \cdot 0.1^2 (7.31 \cdot 10^{-6})^2} = 1.041 \cdot 10^{-6}.$$

Second revolution.

1) Find the sum of the parameters of preload and transverse feed:

$$\Delta A_2 = S_y + N = 5 \cdot 10^{-6} + 10 \cdot 10^{-6} = 15 \cdot 10^{-6}\text{, m.}$$

2) Determine the depth of micro-cutting:

$$t_{f2} = S_y + t_{f1} = 5 \cdot 10^{-6} + 14.91 \cdot 10^{-6} = 19.91 \cdot 10^{-6}\text{, m.}$$

3) Calculate the value of the radial removal of the material at the current turn:

$$\Delta r_{\omega 2} = \frac{(19.91 \cdot 10^{-6})^2}{\frac{7\pi}{15} 19.91 \cdot 10^{-6} + \frac{13\pi}{3} \frac{0.25}{0.85(35 + 0.25) 15.866 \cdot 10^6 \sqrt{0.1 \cdot 7.31 \cdot 10^{-6}}} + \left| 0.24 \cdot 10^{-12} \right|^{0.4}} = 8.513 \cdot 10^{-6}, \text{ m.}$$

4) Calculate the thickness of the layer, in which the roughness is located:

$$H_2 = t_{f2} - \Delta r_{2\omega} = 19,91 \cdot 10^{-6} - 8,513 \cdot 10^{-6} = 11,4 \cdot 10^{-6}, \text{ m.}$$

5) The cutting load at the current speed is equal to:

$$P_{y2} = 3\sqrt{2} \cdot 25 \cdot 10^{-3} \cdot 15.866 \cdot 10^6 \cdot \sqrt{7.31 \cdot 10^{-6} \cdot 10 \cdot 10^{-6} \cdot 11.4 \cdot 10^{-6} \cdot 0.1} \times$$
$$\times \left(0.055 \cdot 11.4 \cdot 10^{-6} \cdot \frac{0.3746}{0.5591} + 0.061 \sqrt{7.31 \cdot 10^{-6} \cdot 10 \cdot 10^{-6}} \right) \cdot 13.33 \cdot 10^8 = 3.789, \text{ N.}$$

6) More precise definition of the values of Δt_{f2}, Δr_2, ΔP_{y2}.

Increment of elastic deformations is:

$$\Delta A_{y2} = \omega_{TS} \cdot \Delta P_y = \omega_{TS} \cdot (P_{y2} - P_{y1}) = 30 \cdot 10^{-9} \cdot (3.789 - 2.884) = 2.716 \cdot 10^{-8}, \text{ m.}$$

Tool wear at the current revolution can be calculated by the equation:

$$\Delta R_i = 0.1 \cdot t_{fi-1}, \tag{9}$$

After substituting the values into equation (9) we have:

$$\Delta R_2 = 0.1 \cdot t_{f1} = 0.1 \cdot 14.91 \cdot 10^{-6} = 14.91 \cdot 10^{-7}, \text{ m.}$$

From equation (1) we determine the increment of the depth of micro-cutting:

$$\Delta t_{f2} = \Delta A_2 - \Delta A_{y2} + \Delta R_2 - \Delta r_{\omega 1} = 15 \cdot 10^{-6} - 2.716 \cdot 10^{-8} + 14.91 \cdot 10^{-7} - 5.844 \cdot 10^{-6} = 10.62 \cdot 10^{-6}, \text{ m}$$

Calculate the value of the depth of micro-cutting:

$$t_{f2} = t_{f1} + \Delta t_{f2} = 14.91 \cdot 10^{-6} + 10.62 \cdot 10^{-6} = 25.53 \cdot 10^{-6}, \text{ m}$$

Radial material removal:

$$\Delta r_{\omega 2} = \frac{(25.53 \cdot 10^{-6})^2}{\frac{7\pi}{15} 25.53 \cdot 10^{-6} + \frac{13\pi}{3} \frac{0.25}{0.85(35 + 0.25) 15.866 \cdot 10^6 \sqrt{0.1 \cdot 7.31 \cdot 10^{-6}}} + \left| 0.28 \cdot 10^{-12} \right|^{0.4}} = 11.79 \cdot 10^{-6}, \text{ m.}$$

The thickness of the layer, in which the roughness is located, is equal to:

$$H_2 = t_{f2} - \Delta r_{\omega 2} = 25.53 \cdot 10^{-6} - 11.79 \cdot 10^{-6} = 13.74 \cdot 10^{-6}, \text{ m}$$

The cutting load is:

$$P_{y2} = 3\sqrt{2} \cdot 25 \cdot 10^{-3} \cdot 15.866 \cdot 10^6 \sqrt{7.31 \cdot 10^{-6} \cdot 10 \cdot 10^{-6} \cdot 13.74 \cdot 10^{-6} \cdot 0.1} \times$$

$$\times \left(0.055 \cdot 13.74 \cdot 10^{-6} \cdot \frac{0.3746}{0.5591} + 0.061 \sqrt{7.31 \cdot 10^{-6} \cdot 10 \cdot 10^{-6}} \right) 13.33 \cdot 10^8 = 4.774, \text{ N.}$$

6) The distance from the deepest valley to the midline of the profile:

$$W_{m2} = \frac{t_{f2} - \Delta r_{\omega 2}}{2} = \frac{25.53 \cdot 10^{-6} - 11.79 \cdot 10^{-6}}{2} = 6.87 \cdot 10^{-6}, \text{ m.}$$

Compare the values W_{m2} and $\Delta r_{\omega 2}$,

$$W_{m2} \le \Delta r_{\omega 2},$$

$$6.87 \times 10^{-6} \le 11.79 \cdot 10^{-6},$$

therefore, in the same way as in the previous revolution, we calculate the value of the arithmetic mean length of the profile R_a, m:

$$R_a = \frac{0.25 V_u^{\,0.4} t_{f2}^{\,0.6}}{K_c (V_u + V_k)^{0.4} n_g^{\,0.4} D_e^{\,0.2} \rho_g^{\,0.2}} =$$

$$= \frac{0.25 \cdot 0.25^{0.4} (25.53 \cdot 10^{-6})^{0.6}}{0.85^{0.4} (0.25 + 35)^{0.4} (15.866 \cdot 10^{6}) \cdot 0.1^{2} (7.31 \cdot 10^{-6})^{2}} = 1.438 \cdot 10^{-6}.$$

For subsequent revolutions of the embedding stage and the steady-state processing mode (S_y = const), the balance of the system is calculated according to the above methodology.

No feed mode.

There is no transverse feed at this stage $S_y = 0$ and preload $N = 0$ [15]. But due to elastic deformations, the grains still cutting-in and, consequently, the metal is being removed $t_{fs} > 0$.

The first turn.

1) The amount of preload and transverse feed is:

$$\Delta A_{N.1} = S + N = 0 + 0 = 0, \text{ m.}$$

2) Tool wear is:

$$\Delta R_{N.1} = 0{,}1 \cdot t_{f\_St.} = 0.1 \cdot 35.52 \cdot 10^{-6} = 35.52 \cdot 10^{-7}, \text{ m.}$$

3) Increment of elastic deformations is:

$$\Delta A_{y\_St.1} = \omega_{TS} \cdot \Delta P_y = \omega_{TS} \cdot (P_{y\_St.10} - P_{y\_St.9}) = 30 \cdot 10^{-9} \cdot (6.257 - 6.257) = 0, \text{ m.}$$

4) Increment of the micro-cutting depth is:

$$\Delta t_{f\_N.1} = \Delta A_{N.1} - \Delta A_{y\_St.1} + \Delta R_{N.1} - \Delta r_{\omega\_St.10} = 0 - 0 + 35.52 \cdot 10^{-7} - 18.52 \cdot 10^{-6} = -14.97 \cdot 10^{-6}, \text{ m.}$$

5) The depth of micro-cutting is determined as:

$$t_{f\_N.1} = t_{f\_St.} + \Delta t_{f\_N.1} = 35.52 \cdot 10^{-6} - 14.97 \cdot 10^{-6} = 20.55 \cdot 10^{-6}, \text{ m.}$$

6) Radial material removal is:

$$\Delta r_{\omega\_N.1} = \frac{(20.55 \cdot 10^{-6})^2}{\frac{7\pi}{15} 20.55 \cdot 10^{-6} + \frac{13\pi}{3} \frac{0.25}{0.85(35+0.25)15.866 \cdot 10^{6} \sqrt{0.1 \cdot 7.31 \cdot 10^{-6}}} + \left|0.25 \cdot 10^{-12}\right|^{0.4}} = 8.867 \cdot 10^{-6}, \text{ m}$$

7) The thickness of the layer, in which the roughness is located, is equal to:

$$H_{N.1} = t_{f\_N.1} - \Delta r_{\omega\_N.1} = 20.55 \cdot 10^{-6} - 8.867 \cdot 10^{-6} = 11.68 \cdot 10^{-6}, \text{ m.}$$

8) The cutting load is:

$$P_{y\_N.1} = 3\sqrt{2}\cdot 25\cdot 10^{-3}\cdot 15.866\cdot 10^{6}\cdot\sqrt{7.31\cdot 10^{-6}\cdot 10\cdot 10^{-6}\cdot 11.68\cdot 10^{-6}\cdot 0.1}\times$$

$$\times\left(0.055\cdot 11.68\cdot 10^{-6}\cdot\frac{0.3746}{0.5591}+0.061\sqrt{7.31\cdot 10^{-6}\cdot 10\cdot 10^{-6}}\right)\cdot 13.33\cdot 10^{8} = 3.902\text{, N.}$$

9) The value of the distance from the deepest valley to the midline of the profile is:

$$W_{m\_N.1} = \frac{t_{f\_N.1}-\Delta r_{\omega\_N.1}}{2} = \frac{20.55\cdot 10^{-6}-8.867\cdot 10^{-6}}{2} = 5.84\cdot 10^{-6}\text{, m.}$$

Compare the values $W_{m\_N.1}$ and $\Delta r_{\_N.1}$,

$$W_{m\_N.1} \le \Delta r_{\omega\_N.1},$$

$$5.84\times 10^{-6} < 8.867\times 10^{-6}.$$

Due to the fact that the value of $\Delta r_{\omega\_N.1}$ is more than the value of $W_{m\_N.1}$, the value of the arithmetic mean length of the profile R_a, m:

$$R_a = \frac{0,25V_u^{0.4}t_{f1}^{0.6}}{K_c(V_u+V_k)^{0.4}n_g^{0.4}D_e^{0.2}\rho_g^{0.2}} =$$

$$= \frac{0,25\cdot 0,25^{0,4}\cdot(20,55\cdot 10^{-6})^{0,6}}{0.85^{0.4}(0.25+35)^{0.4}(15.866\cdot 10^{6})0.1^{2}(7.31\cdot 10^{-6})^{2}} = 1.262\cdot 10^{-6}.$$

The modes calculation continues until the value of the specified roughness $R_a = 0.81\cdot 10^{-6}$ (m) is reached. The calculated data are given in Table 1: *Pl.* – plunge mode, *St.* – steady mode, *N.* – no feed mode.

Table 1

Calculated data

No.	Δt_{fi}	t_{fi}	ΔR_i	$\Delta r_{\omega i-1}$	ΔA_{yi}	H_i
1	2	3	4	5	6	7
Pl. 1	$14.91\cdot 10^{-6}$	$14.91\cdot 10^{-6}$	0	0	$8.698\cdot 10^{-8}$	$9.069\cdot 10^{-6}$
Pl. 2	$10.62\cdot 10^{-6}$	$25.53\cdot 10^{-6}$	$1.491\cdot 10^{-6}$	$5.884\cdot 10^{-6}$	$2.716\cdot 10^{-8}$	$13.74\cdot 10^{-6}$
Pl. 3	$5.737\cdot 10^{-6}$	$31.27\cdot 10^{-6}$	$2.553\cdot 10^{-6}$	$11.79\cdot 10^{-6}$	$2.413\cdot 10^{-8}$	$15.78\cdot 10^{-6}$
Pl. 4	$2.617\cdot 10^{-6}$	$33.89\cdot 10^{-6}$	$3.127\cdot 10^{-6}$	$15.49\cdot 10^{-6}$	$1.964\cdot 10^{-8}$	$16.56\cdot 10^{-6}$
Pl. 5	$1.05\cdot 10^{-6}$	$34.94\cdot 10^{-6}$	$3.389\cdot 10^{-6}$	$17.32\cdot 10^{-6}$	$1.595\cdot 10^{-8}$	$16.85\cdot 10^{-6}$
St. 1	$0.389\cdot 10^{-6}$	$35.33\cdot 10^{-6}$	$3.494\cdot 10^{-6}$	$18.09\cdot 10^{-6}$	$1.372\cdot 10^{-8}$	$16.95\cdot 10^{-6}$
St. 2	$0.14\cdot 10^{-6}$	$35.47\cdot 10^{-6}$	$3.53\cdot 10^{-6}$	$18.38\cdot 10^{-6}$	$1.267\cdot 10^{-8}$	$16.98\cdot 10^{-8}$
St. 3	$0.05\cdot 10^{-6}$	$35.52\cdot 10^{-6}$	$3.547\cdot 10^{-6}$	$18.49\cdot 10^{-6}$	$1.225\cdot 10^{-8}$	$16.99\cdot 10^{-6}$
N.1	$-14.97\cdot 10^{-6}$	$20.55\cdot 10^{-6}$	$3.552\cdot 10^{-6}$	$18.52\cdot 10^{-6}$	0	$11.68\cdot 10^{-6}$
N.2	$-6.88\cdot 10^{-6}$	$13.66\cdot 10^{-6}$	$2.055\cdot 10^{-6}$	$8.867\cdot 10^{-6}$	$7.062\cdot 10^{-8}$	$8.451\cdot 10^{-6}$
N.3	$-3.88\cdot 10^{-6}$	$9.78\cdot 10^{-6}$	$1.366\cdot 10^{-6}$	$5.211\cdot 10^{-6}$	$3.737\cdot 10^{-8}$	$6.437\cdot 10^{-6}$
				$3.343\cdot 10^{-6}$		

The data obtained show that at the stage of the steady-state process, the value of the actual depth of micro-cutting varies according to the harmonic law and is not a constant value ($\Delta t_{fi} \neq 0$) in contrast to what is recommended to be taken in the classical calculation method [16].

The results of the calculations were verified by comparing the calculated and experimental data.

Grinding was carried out on a *Knuth RSM 500 CNC* machine, characterized by increased vibration resistance to external influences. **Initial data:** the material of the workpiece is titanium alloy *VT3*, d = 150 mm, grinding head *AW 60×25×13 63C F90 M 7 B A 35 m/s* , circumferential speed of the wheel V_k = 35m/s, workpiece speed V_u = 0.25 m/s, radial feed S_{yi} = 0.005 mm/r, number of grains per unit area n_g = = $15.86 \cdot 10^6$ pcs/m^2, corner radius the grain vertex $\rho_g = 7.31 \cdot 10^{-6}$ m).

After processing the profilograms taken from the machined blanks, the relative error of the calculated data with the results of the experiment was calculated. The data are summarized in Table 2.

Table 2

Relative error of calculations

No.	t_{fi}	$\Delta r_{\omega i-1}$	H_i		Relative error $\delta_H = \frac{\Delta H}{H_{\exp}} 100\ \%$, %
			calculated	experimental	
Pl. 1	$14.91 \cdot 10^{-6}$	0	$9.069 \cdot 10^{-6}$	$8.16 \cdot 10^{-6}$	11.13
Pl. 2	$25.53 \cdot 10^{-6}$	$5.884 \cdot 10^{-6}$	$13.74 \cdot 10^{-6}$	$12.53 \cdot 10^{-6}$	9.6
Pl. 3	$31.27 \cdot 10^{-6}$	$11.79 \cdot 10^{-6}$	$15.78 \cdot 10^{-6}$	$17.82 \cdot 10^{-6}$	11.45
Pl. 4	$33.89 \cdot 10^{-6}$	$15.49 \cdot 10^{-6}$	$16.56 \cdot 10^{-6}$	$18.88 \cdot 10^{-6}$	12.29
Pl. 5	$34.94 \cdot 10^{-6}$	$17.32 \cdot 10^{-6}$	$16.85 \cdot 10^{-6}$	$19.87 \cdot 10^{-6}$	15.2
St. 1	$35.33 \cdot 10^{-6}$	$18.09 \cdot 10^{-6}$	$16.95 \cdot 10^{-6}$	$19.9 \cdot 10^{-6}$	14.82
St. 2	$35.47 \cdot 10^{-6}$	$18.38 \cdot 10^{-6}$	$16.98 \cdot 10^{-8}$	$19.94 \cdot 10^{-6}$	14.84
St. 3	$35.52 \cdot 10^{-6}$	$18.49 \cdot 10^{-6}$	$16.99 \cdot 10^{-6}$	$19.97 \cdot 10^{-6}$	14.92
N.1	$20.55 \cdot 10^{-6}$	$18.52 \cdot 10^{-6}$	$11.68 \cdot 10^{-6}$	$12.73 \cdot 10^{-6}$	8.25
N.2	$13.66 \cdot 10^{-6}$	$8.867 \cdot 10^{-6}$	$8.451 \cdot 10^{-6}$	$9.3 \cdot 10^{-6}$	9.13
N.3	$9.78 \cdot 10^{-6}$	$5.211 \cdot 10^{-6}$	$6.437 \cdot 10^{-6}$	$5.73 \cdot 10^{-6}$	12.34
		$3.343 \cdot 10^{-6}$			

A comparison of the calculated and experimental data indicates that the accepted mathematical models provide high accuracy of calculations (the relative error is less than 15 %) and make it possible to analytically determine the values of the output parameters of the internal grinding process, taking into account the influence of the relative vibration oscillations of the grinding wheel and the workpiece.

Conclusions

The interrelationships of processing modes with the current parameters of the contact zone when grinding precise holes are established, taking into account the mutual fluctuations of the tool and the workpiece, which allow determining the parameters of the system at the output to avoid cost losses, including reducing the number of defective products and time costs. Constructed non-stationary mathematical dependences allow determining cutting modes during the grinding cycle implementation, taking into account the magnitude of relative vibrations and the initial phase.

It is established that instead of a steady process, harmonic oscillations are observed caused by deviations in the shape of the wheel, the intensity of tool wear and other factors, all of the above has a significant impact on the quality of the machined surface.

The obtained models are universal for various characteristics of the tool, however, for a more adequate description of the process, mathematical dependencies are required. These dependences should include tool wear value for various bond types. The aim of the further research is to determine mathematical dependences.

References

1. Kassen G., Werner G. Kinematische Kenngrößen des Schleifvorganges [Kinematic parameters of the grinding process]. *Industrie-Anzeiger = Industry Scoreboard*, 1969, no. 87, pp. 91–95. (In German).

2. Malkin S., Guo C. *Grinding technology: theory and applications of machining with abrasives*. New York, Industrial Press, 2008. 372 p. ISBN 978-0-8311-3247-7.

3. Hou Z.B., Komanduri R. On the mechanics of the grinding process. Pt. 1. Stochastic nature of the grinding process. *International Journal of Machine Tools and Manufacture*, 2003, vol. 43, pp. 1579–1593. DOI: 10.1016/S0890-6955(03)00186-X.

4. Lajmert P., Sikora V., Ostrowski D. A dynamic model of cylindrical plunge grinding process for chatter phenomena investigation. *MATEC Web of Conferences*, 2018, vol. 148, pp. 09004–09008. DOI: 10.1051/matecconf/20181480900.

5. Leonesio M., Parenti P., Cassinari A., Bianchi G., Monn M. A time-domain surface grinding model for dynamic simulation. *Procedia CIRP*, 2012, vol. 4, pp. 166–171. DOI: 10.1016/j.procir.2012.10.030.

6. Zhang N., Kirpitchenko I., Liu D.K. Dynamic model of the grinding process. *Journal of Sound and Vibration*, 2005, vol. 280, pp. 425–432. DOI: 10.1016/j.jsv.2003.12.006.

7. Ahrens M., Damm J., Dagen M., Denkena B., Ortmaier T. Estimation of dynamic grinding wheel wear in plunge grinding. *Procedia CIRP*, 2017, vol. 58, pp. 422–427. DOI: 10.1016/j.procir.2017.03.247.

8. Garitaonandia I., Fernandes M.H., Albizuri J. Dynamic model of a centerless grinding machine based on an updated FE model. *International Journal of Machine Tools and Manufacture*, 2008, vol. 48, pp. 832–840. DOI: 10.1016/j.ijmachtools.2007.12.001.

9. Tawakolia T., Reinecke H., Vesali A. An experimental study on the dynamic behavior of grinding wheels in high efficiency deep grinding. *Procedia CIRP*, 2012, vol. 1, pp. 382–387. DOI: 10.1016/j.procir.2012.04.068.

10. Jung J., Kim P., Kim H., Seok J. Dynamic modeling and simulation of a nonlinear, non-autonomous grinding system considering spatially periodic waviness on workpiece surface. *Simulation Modeling Practice and Theory*, 2015, vol. 57, pp. 88–99. DOI: 10.1016/j.simpat.2015.06.005.

11. Yu H., Wang J., Lu Y. Modeling and analysis of dynamic cutting points density of the grinding wheel with an abrasive phyllotactic pattern. *The International Journal of Advanced Manufacturing Technology*, 2016, vol. 86, pp. 1933–1943. DOI: 10.1007/s00170-015-8262-0.

12. Guo J. Surface roughness prediction by combining static and dynamic features in cylindrical traverse grinding. *The International Journal of Advanced Manufacturing Technology*, 2014, vol. 75, pp. 1245–1252. DOI: 10.1007/s00170-014-6189-5.

13. Brozgol' I.M. Vliyanie mikrogeometrii poverkhnosti i metoda okonchatel'noi obrabotki dorozhek kacheniya kolets na dolgovechnost' sharikovykh podshipnikov [Influence of surface microgeometry and the method of finishing the raceways of rings on the durability of ball bearings]. *Tekhnologiya podshipnikostroeniya* [Bearing Engineering Technology]. Moscow, 1958, no. 17, pp. 118–125.

14. Korolev A.V. *Issledovanie protsessov obrazovaniya poverkhnostei instrumenta i detali pri abrazivnoi obrabotke* [Investigation of the processes of formation of tool and workpiece surfaces during abrasive processing]. Saratov, Saratov University Publ., 1975. 202 p.

15. Maslov E.N. *Teoriya shlifovaniya materialov* [Theory of materials grinding]. Moscow, Mashinostroenie Publ., 1974. 320 p.

16. Novoselov Yu.K. *Dinamika formoobrazovaniya poverkhnostei pri abrazivnoi obrabotke* [Dynamics of surface shaping during abrasive processing]. Sevastopol, SevNTU Publ., 2012. 304 p. ISBN 978-617-612-051-3.

17. Nosenko V.A., Nosenko S.V. *Tekhnologiya shlifovaniya metallov* [Technology of metal grinding]. 2nd ed. Stary Oskol, Tonkie naukoemkie tekhnologii Publ., 2019. 616 p.

18. Vitenberg Yu.R. Primenenie korrelyatsionnoi teorii dlya otsenki shlifovannoi poverkhnosti [Application of the correlation theory to evaluate the polished surface]. *Vestnik mashinostroeniya = Soviet Engineering Research*, 1969, iss. 1, pp. 55–57. (In Russian).

19. Linnik Yu.V., Khusu A.P. Matematiko-staticheskoe opisanie nerovnostei profilya poverkhnosti pri shlifovanii [Mathematical and static description of surface profile irregularities during grinding]. *Inzhenernyi sbornik = Engineering Review*, 1954, vol. 20, pp. 154–159.

20. Popov S.A., Malevskiy N.P., Tereshchenko L.M. *Almazno-abrazivnaya obrabotka metallov i tverdykh splavov* [Diamond-abrasive processing of metals and hard alloys]. Moscow, Mashinostroenie Publ., 1977. 264 p.

21. Shchegolev V.A., Ulanova M.E. *Elastichnye abrazivnye i almaznye instrumenty* [Elastic abrasive and diamond tools]. Leningrad, Mashinostroenie Publ., 1977. 148 p.

22. Khusu A.P., Vitenberg Yu.R., Pal'mov V.A. *Sherokhovatost' poverkhnostei: teoretiko-veroyatnostnyi podkhod* [Roughness of surfaces: a probabilistic approach]. Moscow, Nauka Publ., 1975. 344 p.

23. Okamura K., Nakajima T. Elastic properties of grinding weel. *Memories of the Faculty of Engineering*, *Kyoto University*, 1969, vol. 31, pt. 4, pp. 490–517.

24. Stadnik T.V. *Povyshenie effektivnosti obrabotki dlinnomernykh tsilindricheskikh zagotovok iz alyuminievykh i titanovykh splavov na operatsiyakh lentochnogo rotatsionnogo shlifovaniya.* Diss. kand. tekhn. nauk. [Improving the efficiency of processing long cylindrical workpieces on aluminum and titanium alloys in operations of belt rotary grinding. PhD eng. sci. diss.]. Sevastopol, 2022. 198 p.

25. Bratan S.M., Chasovitina A.S. Modelirovanie vliyaniya otnositel'nykh vibratsii instrumenta i zagotovki na s"em materiala pri vnutrennem shlifovanii [Modelling of tool and piece part relative motion effect on material removal in internal cylindrical grinding]. *Naukoemkie tekhnologii v mashinostroenii = Science Intensive Technologies in Mechanical Engineering*, 2022, no. 9 (135), pp. 3–9. DOI: 10.30987/2223-4608-2022-9-3-9.

26. Bratan S.M., Roshchupkin S.I., Chasovitina A.S., Gupta K. Vliyanie na veroyatnost' udaleniya materiala otnositel'nykh vibratsii abrazivnogo instrumenta i zagotovki pri chistovom shlifovanii [The effect of the relative vibrations of the abrasive tool and the workpiece on the probability of material removing during finishing grinding]. *Obrabotka metallov (tekhnologiya, oborudovanie, instrumenty) = Metal Working and Material Science*, 2022, vol. 24, no. 1, pp. 33–47. DOI: 10.17212/19946309-202224.13347.

27. Bratan S., Roshchupkin S., Chasovitina A. The correlation of movements in the technological system during grinding precise holes. *Materials Science Forum*, 2021, vol. 1037, pp. 384–389. DOI: 10.4028/www.scientific.net/MSF.1037.384.

28. Kharchenko A., Chasovitina A., Bratan S. Modeling of regularities of change in profile sizes and wear areas of abrasive wheel grains during grinding. *Materials Today: Proceedings*, 2021, vol. 38, pt. 4, pp. 2088–2091. DOI: 10.1016/j.matpr.2020.10.154.

Conflicts of Interest

The authors declare no conflict of interest.